5216 *Chem. Mater.* **2010,** *22,* 5216–5221
DOI:10.1021/cm1012119

CHEMISTRY OF MATERIALS
Article

Mechanochemical Synthesis of Metal−Organic Frameworks: A Fast and Facile Approach toward Quantitative Yields and High Specific Surface Areas

Maria Klimakow,[†] Peter Klobes,[†] Andreas F. Thünemann,[†] Klaus Rademann,[‡] and Franziska Emmerling*[,†]

[†]*BAM Federal Institute for Materials Research and Testing, Richard-Willstaetter-Strasse 11, 12489 Berlin, Germany, and* [‡]*Department of Chemistry, Humboldt-University, Brook-Taylor-Strasse 2, 12489 Berlin, Germany*

Received April 29, 2010. Revised Manuscript Received August 2, 2010

The strategy of utilizing mechanochemical synthesis to obtain metal−organic frameworks (MOFs) with high surface areas is demonstrated for two model systems. The compounds HKUST-1 ($Cu_3(BTC)_2$, BTC = 1,3,5-benzenetricarboxylate) and MOF-14 ($Cu_3(BTB)_2$, BTB = 4,4′,4″-benzenetribenzoate) were synthesized by ball milling and characterized by powder X-ray diffraction (XRD), Raman spectroscopy, scanning electron microscopy (SEM) and thermal analysis (DTA/DTG/MS). The specific surface area (SSA) of both compounds was characterized by nitrogen adsorption. To verify these results and to understand how the synthetic conditions influence the pore structure and the surface area, additional small-angle X-ray scattering (SAXS) experiments were carried out. Our investigations confirm that this synthesis approach is a promising alternative method for distinct MOFs. This facile method leads to materials with surface areas of 1713 m^2/g, which is comparable to the highest given values in the literature for the respective compounds.

Introduction

Microporous and mesoporous metal−organic frameworks (MOFs) are a new class of crystalline materials, which are currently of great interest for applications in sorption, separation, catalysis, and sensor technology.[1−4] Their high inherent porosity is a strong driving force in ongoing research. For example, Férey et al. succeeded in the characterization of compound MIL-101 with an estimated Langmuir surface of 5900 m^2/g.[5] In contrast to their inorganic counterparts zeolites, the novel concept of producing tailor-made porous materials by combining knots (metal ions or clusters) and linkers (rigid organic ligands) allows for a rational design of a desired pore size and structural porosity of the materials. Besides the astonishing results obtained in the area of high surface materials, many authors refer to the experimental challenges in reproducing samples of the same quality. An irreproducibility of surface determination and the strong dependence of the surface areas from the synthetic route for a particular MOF frequently hamper their use.[6,7] Common syntheses based on solvothermal methods often lead to the issues of solvent molecules remaining in the network. Because of their template effect, the subsequent solvent removal can cause the collapse of the network.[8,9] Therefore, activation of the material via costly post-treatment is an important issue as reported in recent contributions (see, for example, ref 10).

In this regard the application of mechanochemistry offers a solvent-free access for the preparation of MOFs and appropriate building blocks.[11] In addition, sufficient amounts of pure material for broad range testing can be easily obtained from this method, which is occasionally difficult when using the common synthetic routes. Furthermore, the solid−solid reaction typically produces quantitative yields.[12] This novel way of synthesis leads directly to products in powder form. Hence, the materials are ready for various applications without the need of time-consuming treatments.

Mechanochemistry as an approach for the synthesis for one-, two-, and three-dimensional metal−organic compounds is currently employed by several groups, mainly focusing on the synthesis of new structures.[13−15] The characterization is usually carried out only by comparison of X-ray diffraction (XRD) data with calculated

*Author to whom correspondence should be addressed. E-mail: franziska.emmerling@bam.de.

(1) Yaghi, O. M.; O'Keeffe, M.; Ockwig, N. W.; Chae, H. K.; Eddaoudi, M.; Kim, J. *Nature* **2003**, *423*, 705–714.
(2) Ferey, G. *Chem. Soc. Rev.* **2008**, *37*, 191–214.
(3) Mueller, U.; Schubert, M.; Teich, F.; Puetter, H.; Schierle-Arndt, K.; Pastre, J. *J. Mater. Chem.* **2006**, *16*, 626–636.
(4) Kitagawa, S.; Kitaura, R.; Noro, S. *Angew. Chem., Int. Ed.* **2004**, *43*, 2334–2375.
(5) Ferey, G.; Mellot-Draznieks, C.; Serre, C.; Millange, F.; Dutour, J.; Surble, S.; Margiolaki, I. *Science* **2005**, *309*, 2040–2042.
(6) Panella, B.; Hirscher, M. *Adv. Mater.* **2005**, *17*, 538–541.
(7) Duren, T.; Millange, F.; Ferey, G.; Walton, K. S.; Snurr, R. Q. *J. Phys. Chem. C* **2007**, *111*, 15350–15356.
(8) Kepert, C. J.; Rosseinsky, M. J. *Chem. Commun.* **1999**, 375–376.
(9) Yaghi, O. M.; Li, H. L.; Davis, C.; Richardson, D.; Groy, T. L. *Acc. Chem. Res.* **1998**, *31*, 474–484.
(10) Nelson, A. P.; Farha, O. K.; Mulfort, K. L.; Hupp, J. T. *J. Am. Chem. Soc.* **2009**, *131*, 458–460.
(11) Garay, A. L.; Pichon, A.; James, S. L. *Chem. Soc. Rev.* **2007**, *36*, 846–855.
(12) Kaupp, G.; Schmeyers, J.; Boy, J. *Chemosphere* **2001**, *43*, 55–61.
(13) Pichon, A.; Lazuen-Garay, A.; James, S. L. *CrystEngComm* **2006**, *8*, 211–214.
(14) Braga, D.; Giaffreda, S. L.; Grepioni, F.; Pettersen, A.; Maini, L.; Curzi, M.; Polito, M. *Dalton Trans.* **2006**, 1249–1263.
(15) Braga, D.; Curzi, M.; Johansson, A.; Polito, M.; Rubini, K.; Grepioni, F. *Angew. Chem., Int. Ed.* **2006**, *45*, 142–146.

Published on Web 08/30/2010

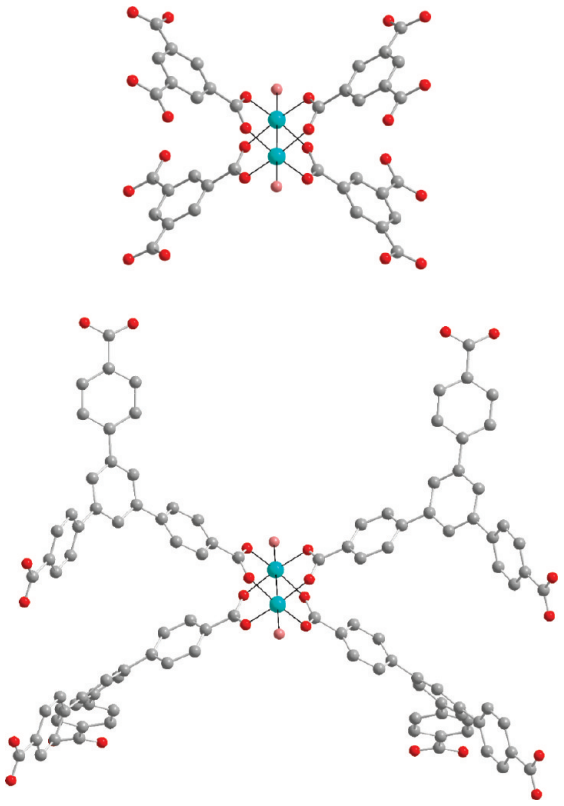

Figure 1. Coordination environment around the dimeric copper unit (so-called paddle wheel) in the crystal structure of HKUST-1 (top) and MOF-14 (bottom); H atoms are omitted for clarity. Color code: Cu atoms, blue; C atoms, gray; O atoms, red; O atoms of water removed upon activation, pale red.

patterns. Further investigations of the properties of these mechanochemically prepared materials in comparison to other synthetic routes are scarce.

In the current contribution we analyze the structural and physical properties of two mechanochemically synthesized MOFs in comparison with traditionally synthesized materials. The intensively studied metal−organic framework HKUST-1[16] ($Cu_3(BTC)_2$, BTC = 1,3,5-benzenetricarboxylate) and its benzenetribenzoate-based analogue MOF-14[17] ($Cu_3(BTB)_2$, BTB = 4,4′,4″-benzenetribenzoate) were chosen as candidate materials for our investigations. Both structures consist of the same copper dimeric paddlewheel unit depicted in Figure 1, which exhibits unsaturated metal centers upon activation. Hence, these materials have gained considerable interest as catalysts and potential adsorbents, because of their high porosity and large specific surface areas (SSAs).[3,18,19] HKUST-1 consists of a non-interwoven cuboctahedral network, whereas MOF-14 has a completely different Pt_3O_4-type topology with two interwoven networks, resulting in a reduced porosity, although the pore diameter (1.6 nm) is larger than that in HKUST-1 (0.9 nm).

The surface area of MOF-14 has only been estimated once as 1502 m^2/g (Langmuir area calculation from the nitrogen adsorption isotherm at 77 K).[17] The experimentally determined values of the surface areas reported for HKUST-1 range from 692 m^2/g to 1944 m^2/g (BET, nitrogen adsorption),[16,20] whereas the majority of values are smaller than 1000 m^2/g, indicating again the severe difficulties concerning the reproducibility of both material quality and measurement. The assumption that the real pore structure and the network of the pores in MOFs deviate from their ideal architecture is a possible explanation for this phenomenon. In this context, SAXS provides information on real pores and their networks from the IUPAC micropore (< 2 nm) to the mesopore scale (2−50 nm).[21] This information may lead to an explanation as to how the synthetic conditions affect the pore structure. In contrast to gas adsorption, small-angle scattering techniques are not affected by closed pores and diffusion barriers.[22] For example, Tsao et al. demonstrated how SAXS can be successfully applied to characterize the pore structure in MOF-5 crystals.[23] Therein, it was shown that the specific surface area (SSA) increases from 800 m^2/g to 3000 m^2/g when the cooling rate is accelerated during crystal formation. Facing the broad range of values for experimentally determined SSAs of one material, the need for further investigation is obvious. It is reasonable to compare the results for a given compound being prepared in different ways by using complementary analytical methods. We investigated the mechanochemically synthesized HKUST-1 (sample **1**) in comparison to samples from electrochemical preparation (sample **2**) and synthesis from ethanolic solution (sample **3**) to determine how the SSA and the pore structure of the different samples depend on the preparation procedure and whether the mechanochemical pathway leads to comparable results.

Experimental Section

Mechanochemical syntheses were carried out in a conventional ball mill via the liquid-assisted grinding of fine powders of copper acetate monohydrate and 1,3,5-benzenetricarbocylic acid (H_3BTC) and copper acetate monohydrate and 4,4′,4″-benzenetribenzoic acid (H_3BTB), respectively, in a molar ratio of 3:2 for 25 min. The color of the powder changed during the reaction from deep green to blue, accompanied by the strong odor of the byproduct, acetic acid (see Scheme 1). Syntheses in ethanolic solution were adopted from Hartmann et al.[24] The electrochemically prepared material is commercially available (BASF, Germany). For explicit descriptions of all experimental details, see the Supporting Information.

(16) Chui, S. S. Y.; Lo, S. M. F.; Charmant, J. P. H.; Orpen, A. G.; Williams, I. D. *Science* **1999**, *283*, 1148–1150.
(17) Chen, B. L.; Eddaoudi, M.; Hyde, S. T.; O'Keeffe, M.; Yaghi, O. M. *Science* **2001**, *291*, 1021–1023.
(18) Alaerts, L.; Seguin, E.; Poelman, H.; Thibault-Starzyk, F.; Jacobs, P. A.; De Vos, D. E. *Chem.—Eur. J.* **2006**, *12*, 7353–7363.
(19) Panella, B.; Hirscher, M.; Putter, H.; Muller, U. *Adv. Funct. Mater.* **2006**, *16*, 520–524.
(20) Wong-Foy, A. G.; Matzger, A. J.; Yaghi, O. M. *J. Am. Chem. Soc.* **2006**, *128*, 3494–3495.
(21) Sing, K. S. W.; Everett, D. H.; Haul, R. A. W.; Moscou, L.; Pierotti, R. A.; Rouquerol, J.; Siemieniewska, T. *Pure Appl. Chem.* **1985**, *57*, 603–619.
(22) Smarsly, B.; Goltner, C.; Antonietti, M.; Ruland, W.; Hoinkis, E. *J. Phys. Chem. B* **2001**, *105*, 831–840.
(23) Tsao, C. S.; Yu, M. S.; Chung, T. Y.; Wu, H. C.; Wang, C. Y.; Chang, K. S.; Chent, H. L. *J. Am. Chem. Soc.* **2007**, *129*, 15997–16004.
(24) Hartmann, M.; Kunz, S.; Himsl, D.; Tangermann, O.; Ernst, S.; Wagener, A. *Langmuir* **2008**, *24*, 8634–8642.

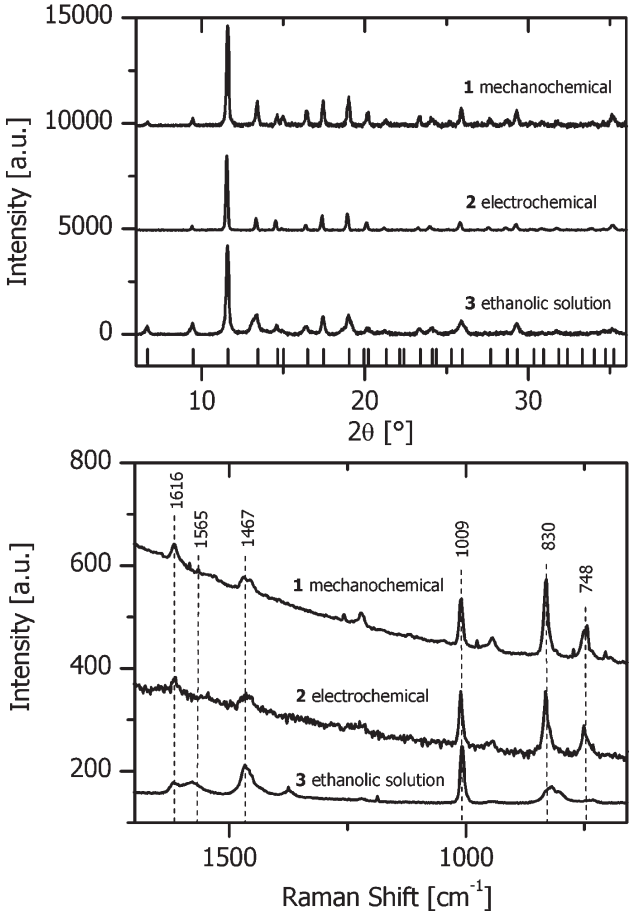

Figure 2. (Top) XRD patterns of samples **1**−**3** synthesized via different routes. Reflections for HKUST-1 calculated from the crystal structure[16] are given for comparison. (Bottom) Raman spectra of samples **1**−**3**.

Scheme 1. Reaction Scheme for the Mechanochemical Syntheses of HKUST-1 and MOF-14

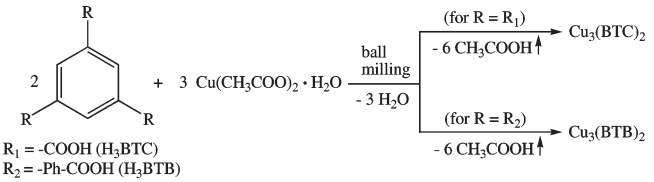

Results and Discussion

In each case, the X-ray diffraction (XRD) patterns and Raman spectra confirmed the completeness of the reaction. The XRD patterns of the HKUST-1 materials synthesized under different conditions are shown in Figure 2. The patterns coincide well among each other and are in good agreement with the theoretical pattern calculated from the crystal structure.[16] The crystallite sizes of samples **1** and **2** derived from the XRD data, calculated using the Debye−Scherrer formula,[25,26] are ∼55 and 50 nm. Sample **3** shows a slight broadening in the reflexes, indicating smaller crystallites

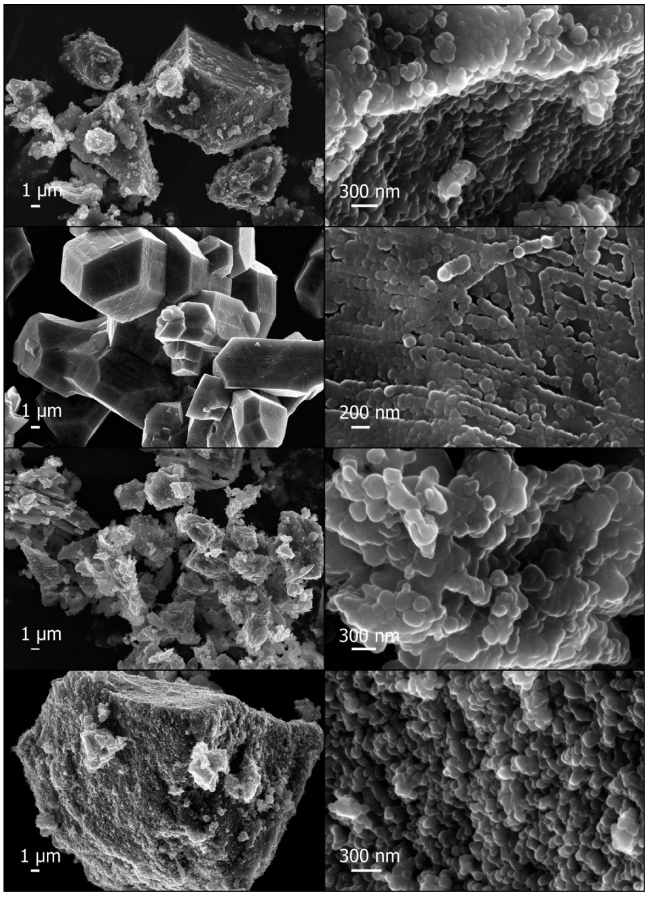

Figure 3. SEM images of dry HKUST-1 powder samples prepared via different synthetic routes (from top to bottom: samples **1**−**4**). The left side shows the particle size distribution and general appearance. The right side depicts the surface of the particles in greater detail.

(31 nm). Figure S1 (see the Supporting Information) shows the diffraction pattern of the mechanochemically prepared MOF-14, which is consistent with the theoretical pattern calculated from the crystal structure.[17]

The Raman spectra of the HKUST-1 powder prepared using different synthetic routes are shown in Figure 2. The spectra obtained are in good agreement with the spectra of HKUST-1 described by Prestipino et al.[27] The vibrational modes of the dimeric copper unit appear in the low-frequency region below 600 cm^{-1}.[28] The bands at 1616 and 1009 cm^{-1} are ascribed to ν(C═C) vibrations of the benzene ring. The symmetric and asymmetric stretching modes of the carboxylate ions can be found at 1467 and 1565 cm^{-1}. The bands at 748 and 830 cm^{-1} are due to out-of-plane bending vibrations of $(C-H)_{ring}$ and to out-of-plane ring bending. In contrast to the mechanochemically and electrochemically prepared samples **1** and **2**, sample **3**, which has been obtained from ethanolic solution, shows a slight peak broadening and lower intensity in several bands. This fact can be explained by the smaller crystallite size for sample **3**.

(25) Scherrer, P. In *Nachrichten von der Gesellschaft der Wissenschaften Göttingen*; Weidmanndsche Buchhandlung: Berlin, 1918; Vol. *2*, pp 98−100.
(26) Klug, H. P.; Alexander, L. E. *X-Ray Diffraction Procedures: For Polycrystalline and Amorphous Materials*, 2nd ed.; Wiley−Interscience: New York, 1974.
(27) Prestipino, C.; Regli, L.; Vitillo, J. G.; Bonino, F.; Damin, A.; Lamberti, C.; Zecchina, A.; Solari, P. L.; Kongshaug, K. O.; Bordiga, S. *Chem. Mater.* **2006**, *18*, 1337–1346.
(28) Holland, P. L.; Cramer, C. J.; Wilkinson, E. C.; Mahapatra, S.; Rodgers, K. R.; Itoh, S.; Taki, M.; Fukuzumi, S.; Que, L.; Tolman, W. B. *J. Am. Chem. Soc.* **2000**, *122*, 792–802.

Table 1. Surface Area (SSA_{BET}) of HKUST-1 Obtained from Different Synthesis Routes

sample	synthesis route	SSA_{BET} [m^2/g]	p/p_0 range for linear BET fit
1	mechanochemical	758	0.004−0.029
2	electrochemical	1836	0.001−0.011
3	ethanolic solution	1184	0.001−0.011
4	mechanochemical and activation	1713	0.005−0.029

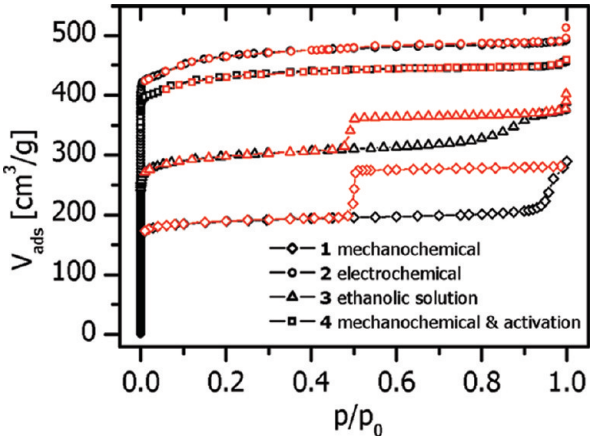

Figure 4. Adsorption (black) and desorption (red) isotherms for nitrogen at 77 K of HKUST-1 samples from different synthetic routes.

The SEM images (depicted in Figure 3) show an inhomogeneous size distribution of the particles and distinct crystal habitus in all HKUST-1 samples.

Mechanochemically synthesized HKUST-1 samples (**1**) without any further cleaning or activation steps show a significantly smaller BET surface area (758 m^2/g), compared to samples **2** and **3** (see Table 1 and Figure 4). Since the XRD patterns were all consistent, there is no indication for differences in the crystal structure (i.e., network interpenetration). It can therefore be assumed that the channels in the structure are blocked or occupied by acetic acid molecules (see Scheme 1) rather than by partial framework collapse. The pore blocking was confirmed by DTA/TG/MS measurements (see Figure S2 in the Supporting Information). The nitrogen isotherms (see Figure 4) of the HKUST-1 samples (**1** and **3**) with considerably smaller surface areas, compared to samples **2** and **4**, are composed of two parts: an initial part with the character of an Type I isotherm and a second part of Type IV isotherm shape showing desorption branches with a pronounced H2 hysteresis loop,[21] which is characteristic for mesopore blocking or cavitation,[29−32] in contrast to the high-surface-area samples, leading to almost-pure Type I isotherms. This phenomenon, connected with capillary condensation that occurs in mesopores, is a hint about the existence of additional mesoporosity. The complete isotherms of mechanochemically prepared MOF-14 show similar mesopore hysteresis loops. (See Figure 8, presented later in this paper.)

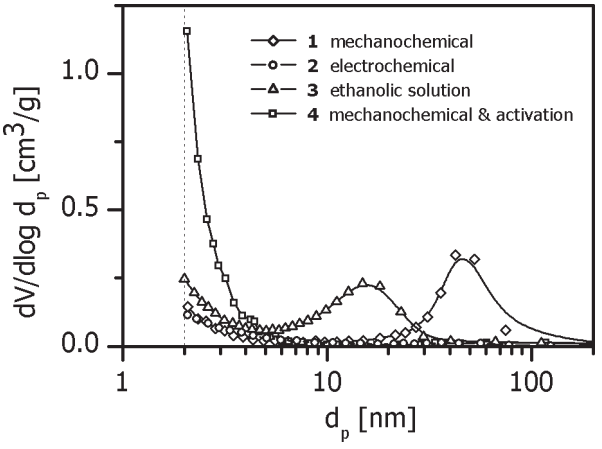

Figure 5. BJH pore size distribution determined from the adsorption branches of the nitrogen isotherms depicted in Figure 4 (the vertical dashed line marks the lower BJH calculation limit at 2 nm).

The assumption of additional mesoporosity in samples **1** and **3** can be corroborated by comparing the pore size distribution of the different samples calculated from gas adsorption measurements using the Barrett−Joyner−Halenda (BJH) method for mesopores.[33] A calculation of the micropore size distribution following the methods of Horvath−Kawazoe[34,35] and Saito-Foley[35] was not carried out, because, for MOF adsorbents, adequate physical parameters for these calculations, such as values for the polarizability and magnetic susceptibility, are still missing in the literature. A similar situation exists for the application of the more-sophisticated Non-Local-Density Functional (NLDFT) approaches for the pore size calculation of MOFs.[36] At present, only a limited number of calculation kernels for more or less ideal adsorption potentials and geometries are available for carbons and zeolite-like materials,[37] but not for MOFs. Recently, a first attempt for applying NLDFT calculations to MIL-101 type MOFs has been made,[38] leading particularly in the range of mesopore filling to a good agreement between the calculated NLDFT isotherm and the experimental adsorption isotherm, although the assumed adsorption potential (N_2-oxidic/siliceous surface) and geometry (cylindrical) was far from the real adsorbent situation. The mesopore distributions for the HKUST-1 samples in this work were calculated using the classical BJH model, which is based on the Kelvin equation.

The BJH pore size calculations[33] (see Figure 5), using the adsorption branches of the nitrogen isotherms in Figure 4, indicate mesopore peaks at pore diameters of ∼45 and ∼15 nm for sample materials **1** and **3**, whereas the BJH pore size distributions of sample materials **2** and **4** with the highest BET areas do not exhibit mesopore peaks. This result only

(29) Sarkisov, L.; Monson, P. A. *Langmuir* **2001**, *17*, 7600–7604.
(30) Ravikovitch, P. I.; Neimark, A. V. *Langmuir* **2002**, *18*, 9830–9837.
(31) Rigby, S. P.; Fletcher, R. S. *J. Phys. Chem. B* **2004**, *108*, 4690–4695.
(32) Thommes, M.; Smarsly, B.; Groenewolt, M.; Ravikovitch, P. I.; Neimark, A. V. *Langmuir* **2006**, *22*, 756–764.
(33) Barrett, E. P.; Joyner, L. G.; Halenda, P. P. *J. Am. Chem. Soc.* **1951**, *73*, 373–380.
(34) Horvath, G.; Kawazoe, K. *J. Chem. Eng. Jpn.* **1983**, *16*, 470–475.
(35) Saito, A.; Foley, H. C. *AIChE J.* **1991**, *37*, 429–436.
(36) Ravikovitch, P. I.; Neimark, A. V. *Colloids Surf. A* **2001**, *187*, 11–21.
(37) Lueking, A. D.; Kim, H. Y.; Jagiello, J.; Bancroft, K.; Johnson, J. K.; Cole, M. W. *J. Low Temp. Phys.* **2009**, *157*, 410–428.
(38) Moellmer, J.; Celer, E. B.; Luebke, R.; Cairns, A. J.; Staudt, R.; Eddaoudi, M.; Thommes, M. *Microporous Mesoporous Mater.* **2010**, *129*, 345–353.

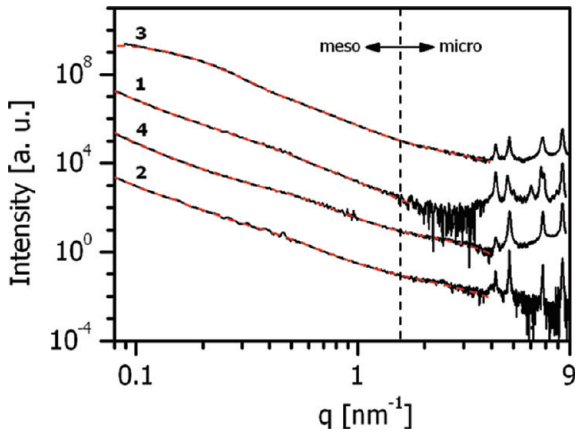

Figure 6. SAXS profiles of different HKUST-1 samples (black trace) and curve approximations according to IFT method (red dashed trace). The intensities of the curves are multiplied by factors of 10^2 (sample **4**), 10^4 (sample **1**), and 10^6 (sample **3**) for clarity of presentation.

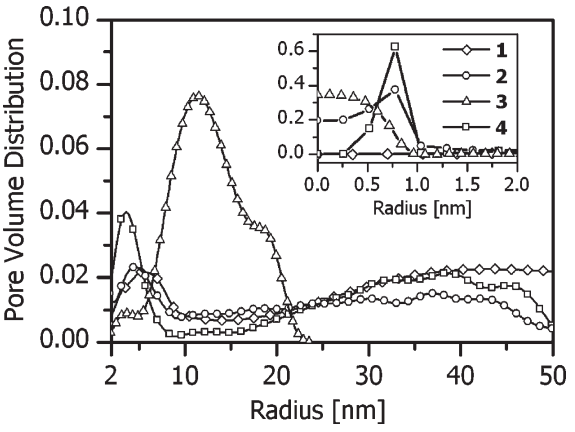

Figure 7. Pore volume distributions of HKUST-1 samples. Inset: magnified view of the micropore region. The curves correspond to the SAXS data approximations shown in Figure 6.

represents the approximate size of the mesopores in sample materials **1** and **3**, because the BJH model represents a macroscopic, thermodynamic method that is not sensitive to details of the adsorption potential and may underestimate the pore sizes by up to 25% for narrow mesopores (pores smaller than 10 nm in width).[39] The mesopores in MOFs such as HKUST-1 are most probably not intrinsic pores in the crystal lattice (e.g., partially collapsed framework regions) but may be due to amorphous domains that are removed upon activation. Such amorphous areas located on the surfaces of the larger MOF crystals are shown in the SEM images of dry HKUST-1 powder samples taken at higher magnification factors (see the images on the right side of Figure 3). The disordered amorphous domains are mostly pronounced for samples **1** and **3**. It seems that, during the activation procedure of the MOFs, as a side effect, the aggregates in the amorphous domains are partially destroyed, leading to the disappearance of the majority of the mesopores and the hysteresis loops. The MOF activation itself consists of removing acetic acid molecules from the MOF nanochannels, making the structural MOF cavities accessible for nitrogen as the BET analysis gas. One possible reason for the formation of disordered amorphous domains with mesoporosity at the surfaces of the MOF crystals of mechanochemically synthesized samples could be a local melting process during the mechanochemical reaction in the ball mill. On the other hand, the presence of such domains also for HKUST-1 samples synthesized via other routes is not clear yet and requires further investigation.

A successful removal of the acetic acid molecules blocking the micropores was achieved upon simply treading the "as synthesized" sample **1** with an ethanol/water mixture (leading to sample **4**). As a result, the SSA was increased by more than 200%, from 758 m^2/g to 1713 m^2/g, reaching values comparable to that of the commercially available sample material **2** of 1836 m^2/g (see Figure 4 and Table 1). In addition, the adsorption−desorption hysteresis vanishes completely after one single activation procedure.

All measured SSA values are below the theoretically calculated maximum accessible surface area of 2153 m^2/g for HKUST-1.[7] The SSA obtained for sample **3** lies within the average range of those determined for other HKUST-1 samples described in the literature.[16,24] The SSAs of samples **2** and **4** are close to the highest values measured so far for nitrogen adsorption onto HKUST-1 samples exposed to air.[20] Therefore, it can be concluded that the pore structure of the mechanochemically synthesized sample is comparable to those obtained electrochemically.

In addition to gas adsorption, the pore structure was measured by small-angle X-ray scattering (SAXS). The SAXS curves of the four HKUST-1 samples synthesized by different routes are shown in Figure 6. Mesopores contribute mainly to the strong intensity increase in the low-q region, up to $\sim$1.5 nm^{-1}, while the form factor of micropores is visible in the medium-q region between 1.5 nm^{-1} and 4.0 nm^{-1}, as indicated by arrows. The first wide-angle reflections of the MOF lattice dominate the curves above 4 nm^{-1} and camouflage the Porod region of the micropores. Therefore, they prevent determination of the SSA by applying Porod's law.[40] Our findings are analogous to the SAXS profiles of MOF-5 crystals reported by Tsao et al.[23]

From inspection of the curve shapes in Figure 6, it is obvious that only the sample prepared from ethanolic solution (sample **3**) bends down at low q-values, resulting from a preferred size of mesopores. In the form factor region of the micropores, it is striking that the intensity of the mechanochemically prepared sample (**1**) is extremely low, i.e., only a continued noisy decay of the mesopore scattering is visible. Obviously, there are no X-ray-visible micropores in sample **1**. This is consistent with the finding of the low value of the SSA by nitrogen adsorption. A possible explanation for this result is that the micropores are filled with acetic acid that was remaining as a byproduct from the synthesis.

A quantitative determination of the pore size distribution is possible by means of the indirect Fourier

(39) Sonnauer, A.; Hoffmann, F.; Froba, M.; Kienle, L.; Duppel, V.; Thommes, M.; Serre, C.; Ferey, G.; Stock, N. *Angew. Chem., Int. Ed.* **2009**, *48*, 3791–3794.

(40) Glatter, O.; Kratky, O. *Small Angle X-ray Scattering*; Academic Press: London, 1982.

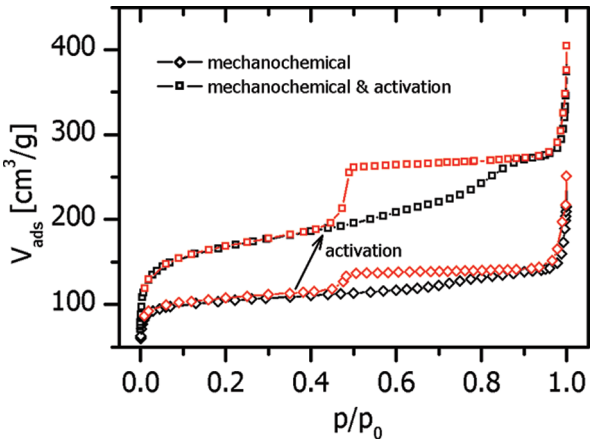

Figure 8. Adsorption (black) and desorption (red) isotherms for nitrogen at 77 K of mechanochemically prepared MOF-14 before and after activation.

transformation (IFT) method.[41] The volume-weighted size distribution of the pores can be computed via this established method by approximating the shape of the pores as spheres, which seems to be a reasonable assumption here. From the calculated scattering pattern (see dashed red lines in Figure 6), the pore volume distributions displayed in Figure 7 are received. An enlarged view of the micropore region is shown in the inset.

A similar pore size distribution in samples **2** and **4** was observed, because of the activation step after the mechanochemical synthesis, cleaning the filled micropores in sample **1**. A distinct maximum is visible for both samples for micropore radii of ~0.8 nm. No distinct maximum of micropores is found for sample **3**.

In the mesopore region, all samples exhibit a maximum in the range of 4−6 nm. This indicates the presence of similar pores in all samples, but with strong differences in their frequency. The frequency of these small mesopores increases in the series of HKUST-1 samples from (a) ethanolic solution, (b) mechanochemical, (c) electrochemical, and (d) mechanochemical and activation synthesis. Here again, the effect of cleaning the 4−6 nm pores in sample **1** leads to an enhancement of the scattering contrast in sample **4**. In the region of mesopores larger than 10 nm, three of the four samples display a broad range of pore sizes up to 40 nm without a preferred size. In contrast, sample **3** has a distinct maximum at 12 nm with a shoulder at 19 nm, but no significant frequency of pores larger than 25 nm.

In comparison to HKUST-1, nitrogen adsorption measurements of mechanochemically prepared MOF-14 showed a SSA of 403 m^2/g. This value increased by more than 150% to a final surface area of 628 m^2/g when the sample was activated with ethanol (see Figure 8). The determined value is significantly smaller than the reported value of 1502 m^2/g;[17] however, this was determined with Langmuir area calculations, which always lead to values higher than BET calculations. Nevertheless, the strong increase of the SSA of MOF-14 after the activation step indicates a general trend of its importance for high-SSA MOFs. The step and the hysteresis in the sorption curves of mechanochemically prepared MOF-14 are due to the existence of additional mesoporosity. Presumably, these effects occur from the mechanochemical synthesis. Surprisingly, the hysteresis loop increases upon activation. Further investigations are necessary to characterize these side effects of our sorption studies.

(41) Glatter, O. *J. Appl. Crystallogr.* **1980**, *13*, 7–11.

Conclusions

In summary, the mechanochemical approach proved to be a reliable and effective strategy for the synthesis of robust metal−organic frameworks (MOFs). As well as being a quick and easy procedure, it offers quantitative yields and materials of high quality. This green-chemistry approach leads to framework structures with easily removable guest molecules, affording a reproducible free pore access for other applications. The one-pot-reaction method enables the synthesis of significant amounts of these compounds, because it can easily be scaled up. The capability of this method was demonstrated for the synthesis of HKUST-1, and its applicability for other MOFs was shown for MOF-14.

The influence of different synthetic procedures on the pore structure and specific surface area (SSA) was investigated, showing that small SSAs correlate to the existence of additional mesoporosity in the materials. The size distribution of the mesopores could be calculated using results from the two different analytical techniques gas adsorption and SAXS. The occurrence of mesopores in the mechanochemically prepared samples correlates with a pore blocking effect, because of the remaining molecules of acetic acid in the framework. Despite this fact, the formation of a gaseous byproduct is a strong driving force for the reaction, leading to quantitative yields. The guest molecules could easily be removed using one single post-synthesis activation step, resulting in a material with a maximized surface area proved by BET and SAXS measurements. We have confirmed the applicability and utility of the mechanochemical synthesis for distinct MOFs; however, there is still great potential for further investigations.

Acknowledgment. We thank A. Zimathies for gas adsorption measurements and S. Rolf for technical assistance. The authors are grateful to B. Unger for performing DTA/DTG/MS measurements, to J. Kneipp for Raman spectroscopy, to E. Labsch for CHN analysis, and to S. Benemann for providing the SEM images.

Supporting Information Available: Detailed experimental procedures, DTA/DTG/MS for HKUST-1, XRD data for MOF-14, and CHN analysis. This material is available free of charge via the Internet at http://pubs.acs.org.